J. Micro/Nanolith. MEMS MOEMS 10(1), 013015 (Jan–Mar 2011)

Multilaboratory comparison of traceable atomic force microscope measurements of a 70-nm grating pitch standard

Ronald Dixson
National Institute of Standards and Technology
100 Bureau Drive
Gaithersburg, Maryland 20899–8212
Email: ronald.dixson@nist.gov

Donald A. Chernoff
Advanced Surface Microscopy
3250 North Post Road, Suite 120
Indianapolis, Indiana 46226

Shihua Wang
National Metrology Centre
A*STAR
1 Science Park Drive
Singapore 118221

Theodore V. Vorburger
National Institute of Standards and Technology
100 Bureau Drive
Gaithersburg, Maryland 20899–8212

Siew-Leng Tan
National Metrology Centre
A*STAR
1 Science Park Drive
Singapore 118221

Ndubuisi G. Orji
Joseph Fu
National Institute of Standards and Technology
100 Bureau Drive
Gaithersburg, Maryland 20899–8212

Abstract. The National Institute of Standards and Technology (NIST), Advanced Surface Microscopy (ASM), and the National Metrology Centre (NMC) of the Agency for Science, Technology, and Research (A*STAR) in Singapore have completed a three-way interlaboratory comparison of traceable pitch measurements using atomic force microscopy (AFM). The specimen being used for this comparison is provided by ASM and consists of SiO_2 lines having a 70-nm pitch patterned on a silicon substrate. For this comparison, NIST used its calibrated atomic force microscope (C-AFM), an AFM with incorporated displacement interferometry, to participate in this comparison. ASM used a commercially available AFM with an open-loop scanner, calibrated with a 144-nm pitch transfer standard. NMC/A*STAR used a large scanning range metrological atomic force microscope with He-Ne laser displacement interferometry incorporated. The three participants have independently established traceability to the SI (International System of Units) meter. The results obtained by the three organizations are in agreement within their expanded uncertainties and at the level of a few parts in 10^4. *© 2011 Society of Photo-Optical Instrumentation Engineers (SPIE).* [DOI: 10.1117/1.3549914]

Subject terms: atomic force microscopes, metrology; pitch; standards; calibration; traceability.

Paper 10111PR received Sep. 20, 2010; revised manuscript received Dec. 16, 2010; accepted for publication Dec. 30, 2010; published online Mar. 8, 2011.

1 Introduction

Traceable pitch standards (gratings) are commonly used to calibrate the magnification of scanning electron microscopes (SEMs) and atomic force microscopes (AFMs) in the *x-y* plane. Beginning in 1998, a series of nano-dimensional metrology comparisons have been conducted among National Metrology Institutes (NMIs) with applicable instruments. Two of these comparisons involved measurement of one- and two-dimensional grating pitches with relatively large values between 290 nm and 1000 nm.[1,2] However, gratings with pitches smaller than 100 nm already exist in semiconductor and data storage products and are produced for research in other areas of nanotechnology, including optics and medicine. The availability of traceable gratings with a pitch smaller than 100 nm will enable more accurate measurement of such structures because a microscopic image is best calibrated using a grating pitch smaller than the image size. That could be why the NMIs of Germany and Japan have recently performed bilateral comparisons of 100-nm, 50-nm, and 25-nm pitch gratings.[3,4]

This paper compares traceable pitch measurements of the same 70 nm pitch grating performed in three different laboratories – including two NMIs – using three different AFMs. The participants in this interlaboratory comparison were the National Institute of Standards and Technology (NIST), Advanced Surface Microscopy (ASM), and the National Metrology Centre (NMC) of the Agency for Science, Technology, and Research (A*STAR) in Singapore. The specimen being used for this comparison was provided by ASM and consists of SiO_2 lines having a 70-nm pitch patterned on a silicon substrate.

1932-5150/2011/$25.00 © 2011 SPIE

Downloaded from SPIE Digital Library on 14 Mar 2011 to 98.226.79.148. Terms of Use: http://spiedl.org/terms

NIST used a custom in-house dimensional metrology AFM, called the calibrated AFM (C-AFM).[5] The NIST C-AFM incorporates interferometric displacement metrology in all three axes to achieve traceability to the International System of Units (SI) meter. ASM used a commercially available AFM with an open-loop scanner, calibrated by a 144 nm pitch transfer standard. In a prior collaboration with Physikalisch-Technische Bundesanstalt (PTB), the German national metrology institute, ASM's transfer standard was calibrated using PTB's traceable optical diffractometry instrument. Thus, ASM's measurements are also traceable to the SI meter.[6] NMC/A*STAR used a large scanning range metrological atomic force microscope (LRM-AFM).[7] The LRM-AFM integrates an AFM scanning head into a nanopositioning stage equipped with three built-in He-Ne laser interferometers so that displacements in all three axes are directly traceable to the SI meter.

In this paper, we describe the instruments and methods used in each lab, the specimen and sampling plan, and the results of the comparison including the uncertainty estimates. Since the details of edge bias and other shape distortions that result from the probe-sample interaction generally cancel out in a pitch (feature spacing) measurement, pitch is a measurand that is largely insensitive to the type of instrument being used (e.g., AFM, SEM, optical microscope). Therefore, the results presented here have applicability to instruments other than AFMs, such as SEMs and optical instruments.

2 Instruments and Methods Used for Measurements

2.1 *NIST Calibrated Atomic Force Microscope*

The NIST C-AFM was constructed to perform traceable dimensional metrology. It is primarily intended to calibrate physical standards for other AFMs. The design, performance, and uncertainties of the system have been discussed elsewhere.[5,8–10] The C-AFM has metrology traceability to the SI meter in all three axes via the 633-nm wavelength of an I_2-stabilized He-Ne laser. The lateral axes are closed-loop controlled using interferometry. The *z*-axis uses a capacitance gauge for real time displacement metrology, and this gauge is calibrated off-line using interferometry. The C-AFM operates in contact mode and performs both pitch and step height measurements.

A scanning sample design was chosen for the C-AFM, largely for the ease of interferometry integration with low Abbe offsets – a few mm in this case. A photograph of the C-AFM metrology frame (holder: see caption) and head is shown in Fig. 1. The composite scanner consists of an *x-y* flexure stage with six degrees of freedom – three translational and three angular, integrated capacitance sensors, and an independent *z*-stage with an integrated capacitance sensor to which the specimen platform is attached. This scanner displaces the specimen platform relative to the metrology frame. Both the lateral interferometer optics and the AFM head are kinematically mounted to the metrology frame. This design permits the lateral axes interferometry to be done in real time, allowing the option of closed-loop position control in the lateral axes.

The *x-y* stage is supplied with a stand alone programmable digital controller that allows for closed-loop operation using the integrated capacitance sensors. Since we use interferometers with our AFM scan controller to independently close the loop, we operate the *x-y* stage itself open-loop with respect to the capacitance gauges for the *x* and *y* axes. However, by using the closed-loop control for the other four degrees of freedom – three tilt angles and the *z*-axis position, we are able to reduce the undesired angular motion of the stage and the resulting lateral axis Abbe errors by three orders of magnitude relative to prior generations of the instrument.[8,10] We were also able to reduce the out-of-plane motion error (i.e., the *z*-straightness of the *x* and *y* axes) to less than 1 nm over the almost 100-μm lateral scan range.

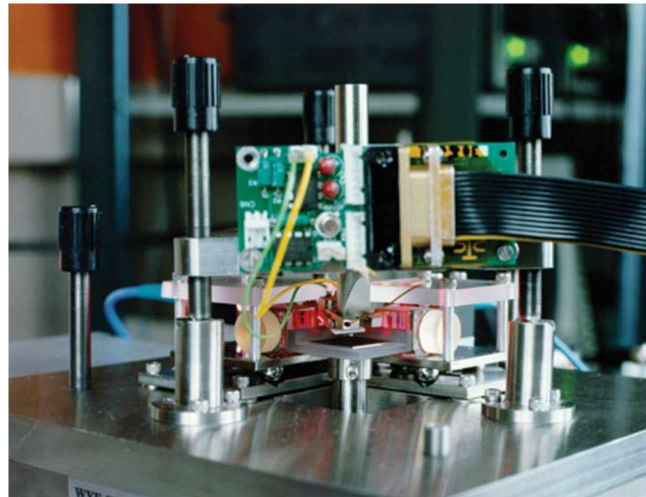

Fig. 1 Side view of the NIST C-AFM showing the AFM head with probe tip positioned just above a wafer chip sample and the metrology frame consisting of a low thermal expansion alloy.

2.2 *Characterized Commercial AFM at ASM*

ASM used a Veeco Metrology/Digital Instruments Dimension 3100* AFM, operated by a NanoScope IIIA controller with Electronics extender module ("phase box"). The open-loop scanner was calibrated to factory specifications. During measurements, the tip is scanning and the sample is stationary. Large and/or massive samples can be examined, as can be seen in Fig. 2. The AFM can operate in both contact and intermittent contact modes – both of which exhibit similar precision. One run in each mode was performed in this work. The images produced by the open-loop scanner are calibrated using images of a 144-nm pitch transfer standard. In a prior collaboration with PTB, the German national metrology institute, ASM's transfer standard was calibrated using PTB's traceable optical diffractometry instrument. Thus, ASM's measurements are also traceable to the SI meter.[6]

An open-loop scanner has the potential advantage that its images are not affected by the sensor noise present in closed-loop systems, but it has the real disadvantage that piezoelectric actuators suffer from nonlinearity and drift. Although the NanoScope controller corrects for most of the

*Certain commercial equipment is identified in this paper to adequately identify the experimental procedure. Such identification does not imply recommendation or endorsement by the National Institute of Standards and Technology, nor does it imply that the equipment identified is necessarily the best available for the purpose.

Downloaded from SPIE Digital Library on 14 Mar 2011 to 98.226.79.148. Terms of Use: http://spiedl.org/terms

Fig. 2 Dimension 3100 AFM at ASM showing the scanner and a large test specimen.

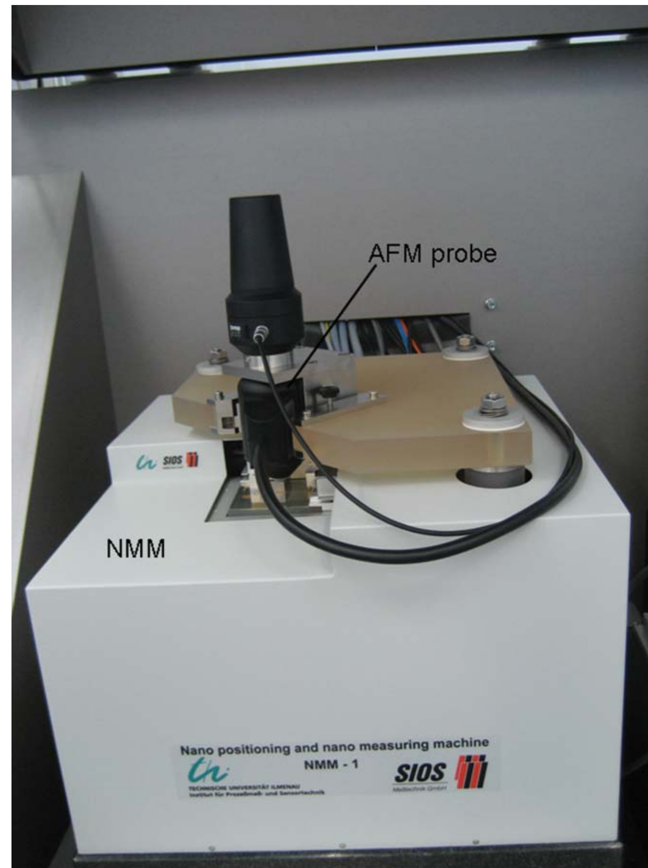

Fig. 3 Photograph of the LRM-AFM at NMC/A*STAR in Singapore.

piezoscanner nonlinearity in real time, residual nonlinearity means that pitch values measured at the edge of an image can differ by 5% from the average value. In addition, the average magnification can change by 1% to 3% during a day. These unfavorable characteristics are overcome here by ASM's data capture and analysis protocols. Both the 70 nm pitch test specimen and the 144 nm pitch transfer standard were placed on the sample stage at the same time and image capture alternated between them. During data analysis, each test image was calibrated using the images preceding and following those of the transfer standard, a procedure that automatically corrects for short term calibration drift. Additional details are given in Sec. 4.

2.3 *Traceable Metrology AFM at NMC/ASTAR*

NMC/A*STAR is using a LRM-AFM.[7] The LRM-AFM, shown in Fig. 3, integrates an AFM scanning head into a nano-positioning stage equipped with three built-in He-Ne laser interferometers so that its measurement related to the motion on all three axes is directly traceable to the SI meter.

The LRM-AFM consists of an AFM probe, a Nano Measuring Machine (NMM), control electronics and software for coordinating servo motion control, signal detection, data acquisition and analysis. An isolation table and an acoustical enclosure are also furnished to minimize the influence of external vibration and noise on the system's performance. The AFM, which is capable of working in intermittent contact mode, was integrated into the NMM. The motions along the three coordinate axes of the NMM were measured by three stabilized He-Ne laser interferometers. The laser frequencies were calibrated by an iodine frequency stabilized laser.

3 Specimen and Sampling Method

3.1 *70-nm Pitch Specimen*

A commercially available 70-nm pitch standard, Model 70-1DUTC (serial number 3555K203) supplied by ASM, was chosen for this comparison. The specimen, a 3 mm × 4 mm silicon chip with ridges of silicon oxide, is mounted on a steel disk for convenience, as shown in Fig. 4 below. The array of ridges covers an area 1.2 mm × 0.5 mm, near the center of the 4 mm × 3 mm chip. The ridge height and width are approximately 35 nm, but these are not the calibrated dimensions. Only the pitch is calibrated. Eleven measurement locations were distributed across the central patterned area of the specimen. A typical AFM scan of this specimen is shown in Fig. 5.

The sampling plan shown in Fig. 4 was used as a guide by the participants, with each laboratory attempting to measure as close to the target location as possible, but avoiding defects as necessary. Each laboratory chose the scanning conditions and image size, and analysis methods depending on the specific strengths of their instruments.

NIST used an image size of 50 μm × 50 μm with 256 scan lines and 4000 points along the fast scan axis; the average data sampling interval was thus 12.5 nm. All data were obtained using contact mode imaging. The analysis used was a frequency domain method in which the peak of the power spectral density is located for each scan line used. The mean pitch for each scan line is then determined from the average peak location.

Downloaded from SPIE Digital Library on 14 Mar 2011 to 98.226.79.148. Terms of Use: http://spiedl.org/terms

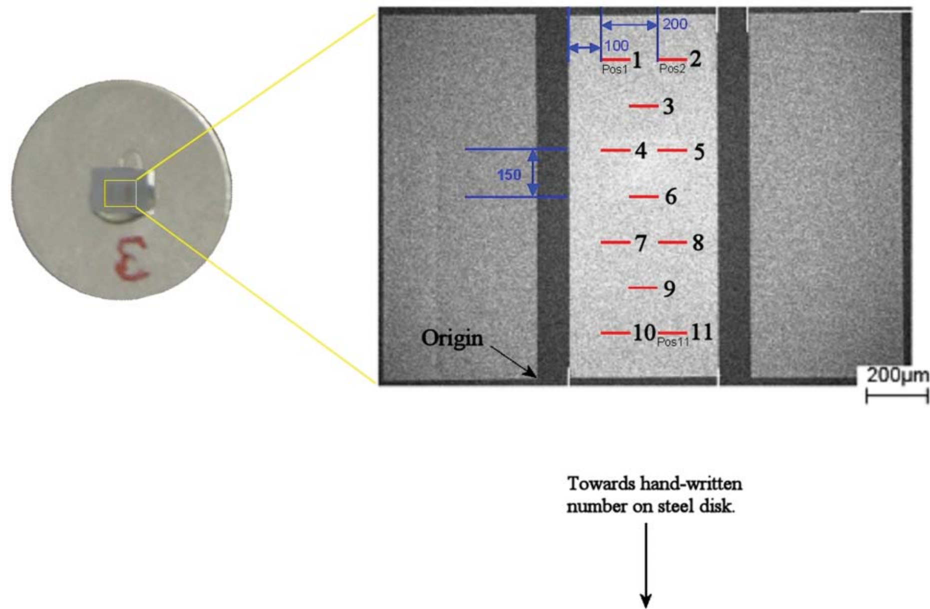

Fig. 4 Picture and layout of sampling plan on 70 nm pitch grating. All dimensions are in μm.

ASM used 3 μm × 3 μm square images with 512 × 512 pixels; the data sampling interval was thus 5.9 nm. The analysis used was a real-space method that extracts the pitch of each interval in the image. Pitch data from the calibration scans that preceded and followed each measurement image of the 70-nm grating were used to correct the pitch results for the comparison specimen. This method mitigates the potential impact of any drift in scale calibration. Individual pitch values are reported for each pair of consecutive ridges in the image. One measurement run used contact mode and one used intermittent contact mode.

NMC/A*STAR used a measurement area of 100 μm × 100 μm at each spot. The images were obtained using intermittent contact mode. The fast scan direction was orthogonal to the ribs of the gratings and the slow axis spacing between profiles was 10 μm. A total of 50 000 data points were captured for each profile; the data sampling interval was thus 2 nm. The measurement data were evaluated using a Fast Fourier Transform method to determine the mean pitch over an effective scanning range of 80 μm.

For all three labs, the final measurement result is the grand average of all the average values obtained from the eleven different measurement positions on the sample.

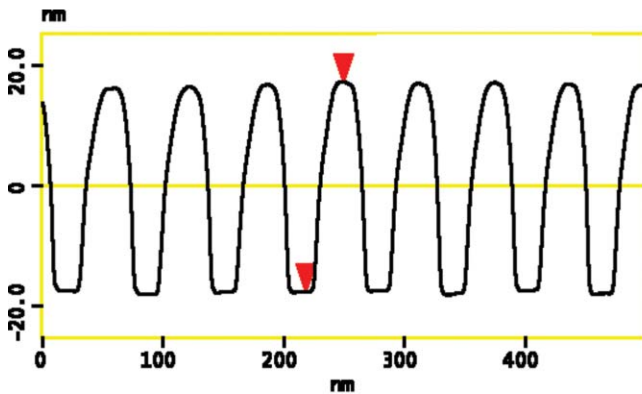

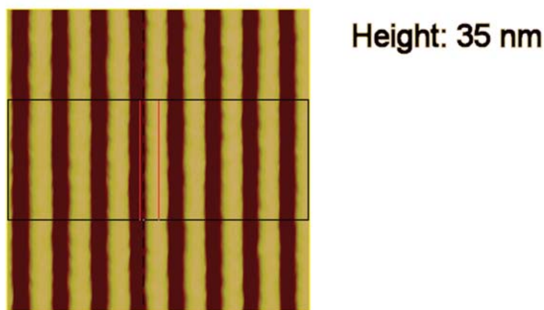

Fig. 5 AFM height image and average profile of the 70 nm pitch standard.

4 Results of Comparison

The overall average pitch values and expanded uncertainties obtained by the participants are shown in Table 1, and

Table 1 Mean pitch values obtained from four measurement runs at three labs, shown in chronological order.

Run	Mean pitch (nm)	Expanded uncertainty (nm) ($k = 2$)
ASM#1	70.071	0.024
NMC	70.072	0.028
NIST	70.055	0.027
ASM#2	70.090	0.021
ASM combined	70.080	0.017

Downloaded from SPIE Digital Library on 14 Mar 2011 to 98.226.79.148. Terms of Use: http://spiedl.org/terms

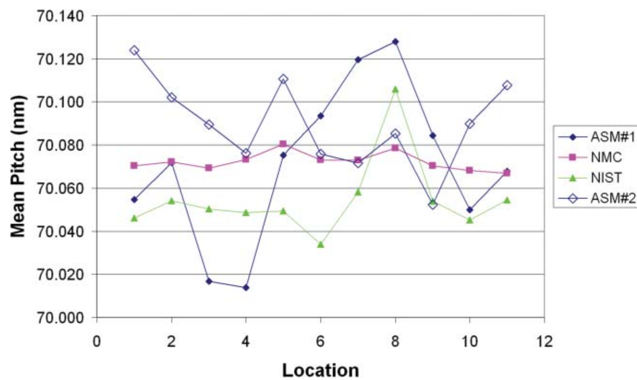

Fig. 6 Mean pitch value of the 70-nm standard by spot, obtained from four measurement runs.

Fig. 6 shows the average pitch values at each of the eleven measurement locations.

The standard approach[11,12] to uncertainty budgets adopted by NMIs such as NIST and NMC/A*STAR is to develop an estimated contribution for every known source of uncertainty in a given measurement and to include terms pertaining to both the instrument used and the particular specimen measured. Terms evaluated exclusively by statistical methods are known as type A components. Terms evaluated using some combination of measured data, physical models, or assumptions about the probability distribution are known as type B components.

This approach was used for our inter-laboratory comparison, with each laboratory developing a draft analysis and uncertainty statement for its own results and then reviewing this analysis with the other participants before publication. In each case, a complete table of uncertainty components is presented, but only the three largest components are discussed in detail.

4.1 *NIST C-AFM Results*

NIST measured the specimen in Oct. 2009 and obtained an average pitch of 70.055 nm $\pm$ 0.027 nm ($k = 2$). The NIST C-AFM images were all 50 μm in scan size and were obtained in contact mode. One image was obtained at each location, except for location 2, where a second image was taken to help assess instrument repeatability. The data set thus includes sampling of grating nonuniformity and instrument variations. Due to particulate contamination at the originally intended location 1, the actual measurement site was moved approximately 100 μm in the direction of location 4.

For each image, the pitch was determined using a frequency domain analysis. An in-house program written in a commercially available data analysis language was used to locate the relevant peak in the power spectral density (PSD). The analysis was performed line by line and the results were then averaged for all of the profiles in an image. The average pitch at each of the eleven locations was shown in Fig. 6. The grand average is given in Table 2.

The estimated value of the measurand is the average of these eleven results, 70.0546 nm. The type A uncertainty, evaluated from the measurements, includes instrument repeatability and reproducibility as well as the effect of sample nonuniformity. It was calculated from the standard deviation of the mean of all eleven results to be 0.0055 nm.

Table 2 Summary of C-AFM pitch results on the 70-1DUTC grating SN203.

Average pitch	70.0546 nm
Standard deviation of 11 locations	0.0182 nm
Standard deviation of the mean	0.0055 nm

4.1.1 *Type B uncertainties in C-AFM pitch measurements*

The type B uncertainties arise from several different sources and were evaluated by various methods. Some of the effects may depend on the sample and on the measurement strategy, such as the number of intervals or locations measured. Three of the type B components listed as potential uncertainties in Table 3 are shown as zero. This is because we consider them to be negligible uncertainties in this particular case, but not necessarily in all cases. These effects must be evaluated for each measurement on a case by case basis.

In general, the sources of uncertainty in C-AFM measurements have been previously discussed.[8,10] Therefore, for brevity, only the three largest components are discussed here. These are the type A contribution from sample nonuniformity and repeatability (which was discussed in Sec. 4.1), the algorithm uncertainty, and the in-plane cosine error.

The first component listed in the type B budget is for the algorithm and measurand definition. For this term, we considered how closely the result calculated from the value calculated from the apparent location of the appropriate peak in the frequency domain, corresponds to the intended measurand of average pitch—as would be determined from the actual location of the peak.

The 70-1DUTC grating specimen has a high level of uniformity across the grating. It is intended for use in scanned probe microscopes and SEMs as a scale calibration reference. Therefore, we regard a frequency domain analysis method, which involves averaging over a significant number of intervals, to be the most relevant for this application, and this was the main focus of our analysis.

For the measurement, the centroid of the PSD peak was calculated using five points centered around the maximum. To estimate the type B uncertainty, the centroids were calculated using one through nine points. The differences observed between the one and nine point calculations were taken to represent extreme results and were used to determine the width of a rectangular distribution that describes the uncertainty associated with this method.

Additionally, for this measurement, the centroids were calculated using a threshold exclusion method to mitigate the contribution of any bad scan lines. The strongest peak was found, and only those scan lines with peak strength above a threshold fraction of this strongest peak were included. Reported results were obtained using 0.5 as the threshold, but the calculation was also performed using 0.25 and 0.75. These results were then taken as the width of the rectangular distribution that describes this contribution to the uncertainty. The standard uncertainties obtained from these two distributions were then added in quadrature to obtain the algorithm standard uncertainty component of 0.0065 nm.

Downloaded from SPIE Digital Library on 14 Mar 2011 to 98.226.79.148. Terms of Use: http://spiedl.org/terms

Table 3 C-AFM Pitch uncertainty budget for 70 nm pitch measurement.

Component	Relative standard uncertainty (proportional contributions)	Standard uncertainty (nm)
Type A		
Repeatability, sample variation (Standard deviation of mean of 11 measured sites)		0.005499
Type B		
Algorithm/measurand definition		0.0065
Laser interferometer, digital resolution		0.0 (included in Type A due to averaging)
Laser interferometer, polarization mixing		0.0 (included in Type A due to averaging)
Laser wavelength in vacuum	1.0×10^{-7}	0.000007
Refractive index of air (temperature, pressure, humidity)	5.1×10^{-6}	0.000357
Deformation/damage of tip		0.0 (included in Type A due to averaging)
Abbe error due to rotation around *z*-axis	2.0×10^{-6}	0.00014
Abbe Error due to rotation around *y*-axis	2.5×10^{-5}	0.00175
Cosine errors (in-sample-plane)	1.5×10^{-4}	0.0105
Cosine errors (out-of-sample-plane)	1.5×10^{-6}	0.000105
Temperature stability (thermal expansion)	7.6×10^{-7}	0.00005320
	Combined standard uncertainty ($k = 1$)	0.0136
	Expanded uncertainty ($k = 2$)	0.0273

The cosine error uncertainties arise from the potential for misalignments among the sample, scanner, and measurement axes. Since misalignments are possible in both the plane of the sample and out of it, we have divided this uncertainty into two terms. Cosine errors for a misalignment in θ approach zero as $\theta^2/2$, so these sources of uncertainty are normally manageable—especially since it is usually possible to estimate the misalignment angle (and correct the result) from the data to an uncertainty of 0.1 deg or less—which would correspond to a relative uncertainty of 1.5×10^{-6} in the measured pitch.

For these measurements, however, the low contrast images increased the difficulty of estimating the misalignment angle. Although direct estimation appeared successful for some images, most could not be corrected to the typical 0.1 deg level. Consequently, we relied on the more conservative estimate of 1 deg misalignment, which roughly corresponds to what is achievable when aligning the sample with the naked eye. As a result, the relative uncertainty of 1.5×10^{-4} due to the in-plane cosine error turned out to be the largest uncertainty contribution. Although this was a disappointing outcome for the present measurements, this source of uncertainty should be readily reducible in similar measurements or future extensions of this work.

4.2 *ASM Results*

ASM measured the specimen in two independent runs – one in contact mode (July 2009) and one in intermittent contact mode (November 2009). The final results for average pitch values were 70.071 nm and 70.090 nm, with expanded uncertainties ($k = 2$) of 0.024 nm and 0.021 nm, respectively. The difference between runs was not statistically significant. The overall average of both runs was 70.080 nm, with expanded uncertainty of 0.017 nm.

In order to appreciate that an open loop AFM can produce accurate results and to estimate the uncertainty, it is necessary to look in detail at the data analysis, where we will see that the most important uncertainty component is the random variation of individual pitch values. The height contrast AFM images were analyzed using ASM's DiscTrack Plus and other software. In a given run of the software, we calculate the pitch using one measured image of the test specimen and two measured images of the calibration standard, one captured before and one captured after the test image. This procedure ("interleaved calibration") increases accuracy by correcting for short term drift in the AFM's magnification and it increases precision by using extra calibration data.

The measurements were made according to procedures described in detail elsewhere[13–15] and summarized here. The software computes an average height profile $Z(x)$ by averaging all scan lines. Peaks on the height profile correspond to ridges (for the 70 nm test specimen) or columns of bumps (for the 144 nm transfer standard). The centroid of each peak is its position. The difference of successive positions is an individual pitch value. No microscope is perfect and Fig. 7(a) shows that there is a significant nonlinearity in the image: apparent pitch values are large at the left side of the image

Downloaded from SPIE Digital Library on 14 Mar 2011 to 98.226.79.148. Terms of Use: http://spiedl.org/terms

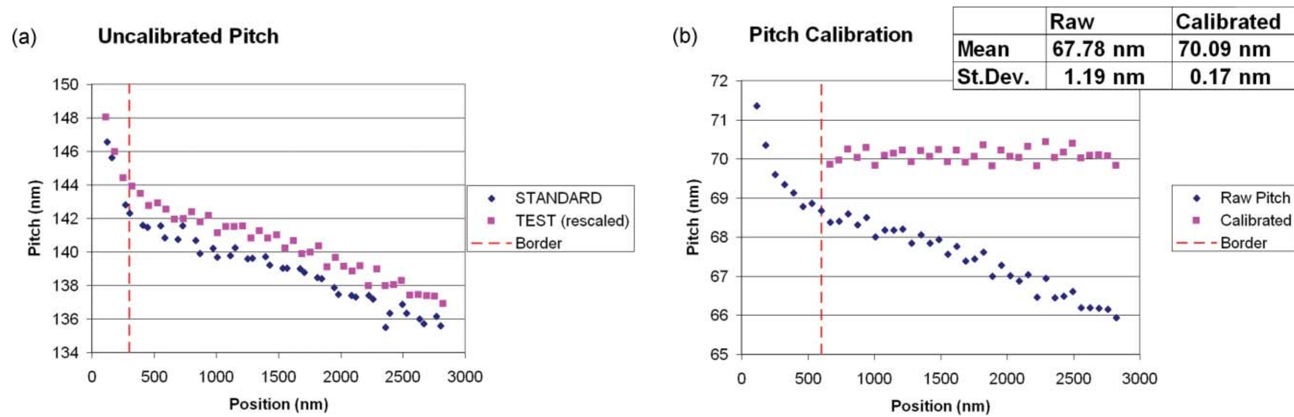

	Raw	Calibrated
Mean	67.78 nm	70.09 nm
St.Dev.	1.19 nm	0.17 nm

Fig. 7 Pitch results for one ASM data set. (a) Raw pitch as a function of position in the image. Points labeled "Standard" are pitch values measured in the calibration images captured before and after the test specimen image. Points labeled "TEST (rescaled)" are pitch values from the test image, which were then multiplied by 2.0535 and offset by 1.5 nm for this graph. The two curves were approximately parallel. (b) Raw and calibrated pitch for the test specimen. The dashed vertical lines indicate data exclusion borders. Because the AFM nonlinearity is hard to correct at the start of scan, we exclude pitch results from the leftmost 20% of the test image and from the leftmost 10% of the calibration images.

(start of scan) and decrease toward the right. Because the image distortion is reproducible from one scan to the next, one can correct this systematic effect in the offline analysis. Using a fifth-order polynomial fit of pitch versus position in the calibration images, the software computes a new length scale that corrects for average magnification error and nonlinearity. The corrected length scale is then applied to the feature position data from the test image to produce a set of corrected pitch values. For this data set, calibration reduced the standard deviation by almost a factor of seven and removed a bias of 3.2% in the mean value (see inset table in Fig. 7).

Because the data analysis is done in real space, each measurement is a single instance of pitch. Knowing the standard deviation of single pitch values can be important for microscopists who calibrate high magnification images containing one or a few pitch intervals. It is also important for estimating the minimum number of measurements needed to achieve a given level of precision for the mean value when performing traceable certification of pitch. In this work, we measured more than 370 pitch values in each run. The pooled standard deviations of single pitch values were 0.20 nm and 0.15 nm for runs 1 and 2, which used contact mode and intermittent contact mode, respectively.

4.2.1 *Uncertainties in ASM measurements*

The expanded uncertainty of single pitch (individual interval) values was 0.40 nm and 0.29 nm for runs 1 and 2, respectively. This uncertainty was dominated by the standard deviation of measured values, which accounted for more than 99% of the overall variance. Note that the uncertainty of individual intervals is of interest to ASM but is much larger than the uncertainty of the average pitch, which was the measurand for this comparison. The uncertainty of single pitch values is thus not further discussed. The uncertainty components of the overall mean value and combined expanded uncertainties for the two ASM measurement runs are shown in Table 4, where they are listed approximately in decreasing order of importance. We first look at the uncertainty components within single runs. These are shown in the columns headed "Run 1" and "Run 2."

Magnification error and image nonlinearity are by far the largest errors present in the original data. We used an Analysis of Variance[16] (ANOVA) calculation to partition the overall variation into two components, called the "within group" and "between group" variances. A natural grouping of the data is by location. Then, the within group variance is the variance of individual pitch values at each location relative to the mean value there, averaged over all locations. The between group variance refers to the variance of mean pitch values for each location relative to the overall mean. The ANOVA result showed that there was no statistically significant difference between images in each run. This is consistent with the impression of random variation given by the graph of mean pitch values in Fig. 6. This means that the interleaved calibration method has successfully corrected for average magnification error. The random variation of pitch values versus position within each image, as shown in Fig. 7(b), indicates that the length scale correction method has successfully corrected for the image nonlinearity. Therefore, we have corrected these effects as fully as is reasonably possible. The remaining random effects contained in the standard deviation of the mean include surface and edge roughness, local pitch variation in the test specimen (whether intrinsic or due to debris on the surface), error in the corrected length scale, tip shape changes, and AFM noise.

The next two uncertainty components have similar importance. The stated uncertainty of the mean pitch of the transfer standard (150-2DUTC) calibrated by optical diffraction at PTB is 0.0075 nm (0.0052%, $k = 1$). Specimen rotation in plane is a type B error. We controlled the rotation of each specimen so that the grating axes were perpendicular to the fast scan direction within 1 deg. Our fundamental measurement is the ratio of the pitch of the test specimen to the pitch of the calibration standard. Rotation of the calibration standard decreases, and rotation of the test specimen increases, the reported pitch of the test specimen. The effect of rotation is proportional to a quotient of cosines, cos(A)/cos(B). With the assumption that the angles A and B have a rectangular distribution in the range -1 to $+1$

Downloaded from SPIE Digital Library on 14 Mar 2011 to 98.226.79.148. Terms of Use: http://spiedl.org/terms

Table 4 ASM's pitch uncertainty budget for 70-1DUTC ($k = 1$). Note: Square picometers (pm^2) are a convenient unit for expressing variances in this table.

	Standard Uncertainty (nm)						
Component	Run 1	Run 2	Run to run correlation coefficient	Covariance (pm^2)	Variance for mean of two runs (pm^2)	Relative variance	Rank
SD of overall mean	0.0104	0.0076	0.0	0	41.6	58.8%	1
Pitch uncertainty of 144-nm standard (standard uncertainty = 0.0075 nm), (relative uncertainty 5.2×10^{-5})	0.0036	0.0036	1	13.32	13.3	18.8%	2
Cosine factor for rotation in plane (0 to 1 deg) (relative uncertainty 6.5×10^{-5})	0.0046	0.0046	0	0	10.4	14.6%	3
Image drift (relative standard uncertainty 1.7×10^{-5} and 5.6×10^{-5}) (depends on scan speed)	0.0012	0.0039	0	0	4.1	5.8%	4
Cosine factor for out of plane tilt (0 to 0.5 deg) (relative uncertainty 1.6×10^{-5})	0.0011	0.0011	1	1.32	1.3	1.9%	5
Combined standard uncertainty (nm)	0.0120	0.0104			0.0084		
Expanded uncertainty, $k = 2$	0.0241	0.0208					
Expanded uncertainty, $k = 2$ for mean of 2 runs	0.0168						

deg, then the mean of the quotient is 1.0 and the standard deviation of the quotient is 0.000 065. This effect gives a constant bias within a given run and contributes to a run to run reproducibility error as specimens are removed and reinserted. The relative standard uncertainty of the run to run error is 6.5×10^{-5}. An additional discussion of cosine errors and resulting uncertainties is given in the Appendix.

Since the various components of uncertainty within a given run are uncorrelated with each other, the combined standard uncertainty is given by the root sum squared of all the uncertainty components. This leads to the expanded uncertainties of 0.0241 nm and 0.0208 nm shown for each single run, respectively.

By combining the results of two runs, we expect to more accurately know the measurand. But computing the combined standard uncertainty is not as simple as dividing the root sum squared of each run's uncertainty by 2.[18] Since the same transfer standard was used in both runs, its pitch uncertainty is a "common mode error" and we show its correlation coefficient as 1.0 in Table 4. Likewise, the cosine factor for out of plane tilt is probably a common mode error, since the sample and AFM mounting are the same. The other uncertainty components have correlation coefficients of 0. For each uncertainty component x, its combined uncertainty U_x when computing the average result from two runs is computed as follows: $V_x = (U_{x1}^2 + U_{x2}^2 + 2* \rho_{x12} * U_{x1} * U_{x2}) /4$, where U_{x1} is the uncertainty of component x in run 1, U_{x2} is the uncertainty of component x in run 2, ρ_{x12} is the run-to-run correlation coefficient, and the expression $\rho_{x12} * U_{x1} * U_{x2}$ is the covariance. Then, $U_x = \sqrt{V_x}$. The correlation coefficient, covariance, and the variance for the mean of two runs are entered in separate columns in Table 4. The overall combined variance is 70.7 pm^2, leading to the expanded uncertainty of 0.0168 nm for the mean of two runs. We can also look at the difference between the two runs. In this case the combined variance for component x is $V_x = (U_{x1}^2 + U_{x2}^2 - 2* \rho_{x12} * U_{x1} * U_{x2})$. Note that now the covariance is subtracted. The resulting expanded uncertainty for the "difference" in pitch values is 0.030 nm, which is greater than the observed difference, 0.019 nm. Therefore, the difference between runs is not statistically significant.

4.3 *NMC/A*STAR Results*

NMC/A*STAR measured the specimen in Aug. 2009 and obtained an average pitch of 70.072 nm ± 0.028 nm ($k = 2$). The NMC/A*STAR data were analyzed using a frequency domain method for each profile at all 11 locations. The results are summarized in Table 5.

Downloaded from SPIE Digital Library on 14 Mar 2011 to 98.226.79.148. Terms of Use: http://spiedl.org/terms

Table 5 Summary of the LRM-AFM measurements at NMC/A*STAR.

Average pitch	70.0723 nm
Standard deviation of 11 locations	0.0042 nm
Standard deviation of the mean	0.0013 nm

4.3.1 *Uncertainties in NMC/A*STAR measurements*

The standard uncertainty evaluated as type A is obtained from a series of measurements on the repeatability and stability of the system. Based on a set of 11 measurement results as shown in Table 5, the type A uncertainty of the pitch measurement of 70.072 nm due to random effects was calculated to be 0.001 27 nm.

The type B uncertainties for the NMC/A*STAR measurements are shown in Table 6. In most cases, a rectangular distribution with the limits stated was used to determine the standard uncertainty component for each effect. Most of the contributions are seen to be negligible.

The largest uncertainty contribution is due to the cosine error arising from potential misalignment of the interferometer axis with the mirror normal. This is followed by the type A contribution, and then the cosine error contribution arising from potential misalignment of the motion and measurement axes.

4.4 *Summary and Comparison*

The final results and uncertainties of the three participants are shown in Table 7. The expanded uncertainties of the participants are comparable and the results are in agreement within these uncertainties. All three participants simultaneously measured and retained a specimen similar to the one used in the comparison, so as to preserve a basis for future improvements. While the offsets observed among the laboratories are within the uncertainties of the comparison, the differences are interesting and will be a subject of further investigation by the participants.

Table 6 Uncertainty budget for the 70-nm grating pitch measurement using the LRM-AFM at NMC/A*STAR.

	Quantity X_i	Relative standard uncertainty	Probability distribution	Sensitivity coefficient c_i	Standard uncertainty $u_{i(P)}$ (nm)	Degrees of freedom ν_i
Type A						
1	Measurement repeatability, R	—	N	—	0.00127	10
Type B						
2	Interferometer data (nonlinearity, resolution) ΔN	0	—	—	Included in type A term due to averaging	—
3	Vacuum frequency, f_0	1.15×10^{-8}	R	70 nm	8.1×10^{-7}	∞
4	Refractive index of air, n	7.1×10^{-7}	N	70 nm	4.97×10^{-5}	∞
5	Cosine error, θ_m	2.0×10^{-4}	R	70 nm	0.014	∞
6	Cosine error, θ_t	2.0×10^{-6}	R	70 nm	0.00014	∞
7	Cosine error, θ_O	3.9×10^{-10}	R	70 nm	2.7×10^{-8}	∞
8	Abbe error, L_{Abbe1}, (rotation around z-axis)	1.0×10^{-6}	R	70 nm	7.0×10^{-5}	∞
9	Abbe error, L_{Abbe2}, (rotation around y-axis)	1.0×10^{-6}	R	70 nm	7.0×10^{-5}	∞
10	Dead path, L_{dp}	0	—	—	Included in type A term due to averaging	—
11	Thermal expansion correction of metrology frame and corner mirror, L_{mf}	1.2×10^{-9}	R	70 nm	8.4×10^{-8}	∞
12	Thermal expansion of sample, L_{ms}	1.8×10^{-7}	R	70 nm	1.26×10^{-5}	∞
	Combined standard uncertainty ($k = 1$)				0.014	∞
	Expanded uncertainty ($k = 2$)				0.028	∞

Downloaded from SPIE Digital Library on 14 Mar 2011 to 98.226.79.148. Terms of Use: http://spiedl.org/terms

Table 7 Comparison of pitch measurements and expanded uncertainties on the 70-nm grating.

Lab	Mean pitch (nm)	Expanded uncertainty (nm)
ASM (two runs)	70.080	0.017
NIST	70.055	0.027
NMC	70.072	0.028

5 Conclusions

NIST, ASM, and NMC/A*STAR have completed a three-way interlaboratory comparison of traceable AFM pitch measurements on a 70 nm pitch grating. The three participants achieved relative expanded uncertainties ($k = 2$) of approximately 4×10^{-4} and their results were in agreement within the uncertainties. All three laboratories are working to improve their capabilities and further refine their uncertainty budgets.

The NIST and NMC/A*STAR results generally demonstrate what can be accomplished in this size regime using instruments with integrated traceable interferometric displacement metrology. Both labs believe that the performance levels of their instruments can be further improved by at least a factor of two. In contrast, the ASM results illustrate that a commercially available AFM can be used to achieve uncertainties at the same level or, in this case, somewhat smaller than the uncertainties achieved with the metrology instruments used by NMIs. However, this approach requires a reference grating on which independent traceable measurements have been performed. In turn, providing traceable measurements could be the province of instruments at NMIs.

Metrology AFMs, such as the NIST C-AFM and the NMC/A*STAR LRM-AFM, are suitable for grating calibration, but other technologies such as SEM and optical diffraction are also capable. For example, the prior collaboration between ASM and PTB involved traceable grating calibration with diffractometry.[6] Diffractometry has the advantage of high throughput relative to AFM, but the pitch that can be measured is limited to about half the source wavelength. The increasing availability of suitable sources with shorter wavelengths, however, suggests that diffractometers will have a role in grating pitch metrology at the nanometer scale. The ongoing development of an extreme ultra-violet scatterometer at PTB (Ref. 17) illustrates the relevance of such methods and of sub-100 nm pitch metrology.

Appendix: Cosine Errors and Uncertainties Due to Sample Rotation

For all three participants, uncertainty due to sample rotation in plane was the largest or second largest component of uncertainty. For this reason, and because cosine errors may be important to other workers in length metrology, we present here the results of numerical simulations of cosine statistics for two different measurement configurations.

In configuration 1, the sample is measured in a calibrated AFM, as was done here by NIST and NMC. The cosine error is computed using the angle θ between the calibrated measurement axis (interferometer axis) and the grating wavevector (the line perpendicular to the ridges). The apparent pitch λ_A of the grating increases with θ by the inverse of the cosine

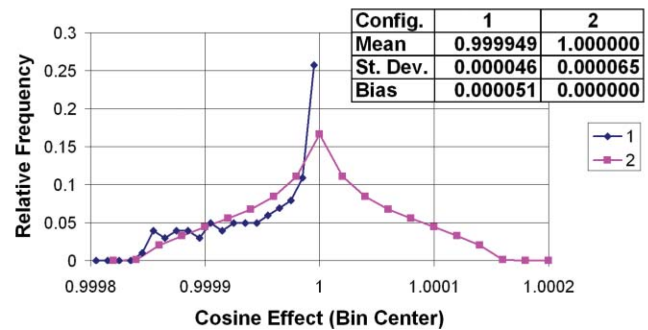

Fig. 8 Cosine effects in configurations 1 and 2. In both cases, the sample rotation in plane relative to the measurement axis is assumed to be a uniform distribution on the interval 0 to 1 deg. Curves 1 and 2 are histograms showing frequency distributions of the functions $1/\cos(\theta)$ and $\cos(\theta_1)/\cos(\theta_2)$, respectively. The inset table shows basic statistics. Note that one configuration is biased and the other is not.

$$\lambda_A = \lambda / \cos(\theta). \tag{1}$$

In a numerical simulation, we tabulated the cosine of each angle from 0 to 1 deg at 0.01 deg increments. This is a uniform (rectangular) distribution in angle. In Fig. 8, curve 1 shows the histogram of cosine values, for 21 bins covering the range 0.9998 to 1, at intervals of 0.00001. Note that the cosine distribution is biased. The mean cosine and its standard deviation are 0.999949 and 0.000046. The sum of the bias (i.e., the offset from unity) plus two standard deviations is 1.43×10^{-4}. This happens to be close to the value of 1.5 $\times\ 10^{-4}$, which was used in the NIST uncertainty budget. The NIST uncertainty model used a conservative estimate as calculated from the difference between the cosine of one degree and unity.

In configuration 2, the sample is measured by comparison with a transfer standard, as was done by ASM. For each object, the apparent pitch increases with θ, the angle between the measurement axis and the grating wave vector. Since the measured pitch involves the ratio of test and standard pitch values, rotation of the calibration standard decreases, and rotation of the test specimen increases, the reported pitch of the test specimen. The cosine factor is now a quotient of cosines, $\cos(\theta_1)/\cos(\theta_2)$. In a numerical simulation, we tabulated 101×101 quotients corresponding to the uniform distribution of each object's angle in the range 0 to 1 deg. In Fig. 8, curve 2 shows the histogram of cosine quotient values, for 21 bins covering the range 0.9998 to 1.0002, at intervals of 0.00002. The mean quotient and its standard deviation are 1.000000 and 0.000065. This standard deviation is used in ASM's uncertainty model. The absence of bias is an advantage of configuration 2.

Acknowledgments

This work was supported in part by the NIST Physical Measurement Laboratory, the management of NMC/A*STAR,

Downloaded from SPIE Digital Library on 14 Mar 2011 to 98.226.79.148. Terms of Use: http://spiedl.org/terms

and internal research funds of ASM. We thank one referee for observing that the uncertainty of the reference grating in ASM's measurements is correlated from run to run.

References

1. F. Meli, "International comparison in the field of nanometrology: pitch of 1D gratings (Nano4)," in *Proceedings of the 2nd Euspen (European Society for Precision Engineering) International Conference*, pp. 358–361, Turin, Italy (2001).
2. J. Garnaes and K. Dirscherl, "NANO5—2D Grating—Final report," *Metrologia* **45**, 04003 (2008).
3. I. Misumi, G. Dai, and G.-S. Peng, "Final report on Supplementary Comparison APMP.L-S2: Bilateral comparison on pitch measurements of nanometric lateral scales (50 nm and 100 nm) between NMIJ/AIST (Japan) and PTB (Germany)," *Metrologia* **44**, 04006 (2007).
4. I. Misumi, G. Dai, M. Lu, O. Sato, K. Sugawara, S. Gonda, T. Takatsuji, H. S. Danzebrink, and L. Koenders, "Bilateral comparison of 25 nm pitch nanometric lateral scales for metrological scanning probe microscopes," *Meas. Sci. Technol.* **21**, 035105 (2010).
5. R. Dixson, N. G. Orji, J. Fu, M. Cresswell, R. Allen, and W. Guthrie, "Traceable Atomic Force Microscope Dimensional Metrology at NIST," *Proc. SPIE* **6152**, 61520P (2006).
6. D. A. Chernoff, E. Buhr, D. Burkhead, and A. Diener, "Picometer-scale accuracy in pitch metrology by optical diffraction and atomic force microscopy," *Proc. SPIE* **6922**, 69223J (2008).
7. S. H. Wang, G. Xu, and S. L. Tan, "Development of a metrological atomic force microscope for nano-scale standards calibration," *Proc. SPIE* **7155**, 71550I (2008).
8. J. A. Kramar, R. Dixson, and N. G. Orji, "Scanning Probe Microscope Dimensional Metrology at NIST," *Meas. Sci. Technol.* **22**, 024001 (2011).
9. R. Dixson, R. Köning, V. W. Tsai, J. Fu, and T. V. Vorburger, "Dimensional Metrology with the NIST calibrated atomic force microscope," *Proc. SPIE* **3677**, 20–34 (1999).
10. R. Dixson, R. Köning, T. V. Vorburger, J. Fu, and V. W. Tsai, "Measurement of pitch and width samples with the NIST calibrated atomic force microscope," *Proc. SPIE* **3332**, 420–432 (1998).
11. *Guide to the Expression of Uncertainty in Measurement* (Geneva: International Organization for Standardization) (1995).
12. B. N. Taylor and C. E. Kuyatt, "Guidelines for Evaluating and Expressing the Uncertainty of NIST Measurement Results," *NIST Tech. Note* 1297 (1994).
13. D. A. Chernoff and D. L. Burkhead, "Automated, high precision measurement of critical dimensions using the Atomic Force Microscope," *J. Vac. Sci. Technol. A* **17**, 1457–1462 (1999).
14. D. A. Chernoff and J. D. Lohr, "High precision calibration and feature measurement system for a scanning probe microscope," U.S. Patent No. 5,644,512 (1997).
15. D. A. Chernoff and J. D. Lohr, "High precision calibration and feature measurement system for a scanning probe microscope," U.S. Patent No. 5,825,670 (1998).
16. G. B. Wetherill, *Elementary Statistical Methods*, p. 263, Methuen & Co., London (1967).
17. G. E. P. Box, W. G. Hunter, and J. S. Hunter, *Statistics for Experimenters*, p. 87, Wiley, New York (1978).
18. F. Scholze, C. Laubis, G. Ulm, U. Dersch, J. Pomplun, S. Burger, and F. Schmidt, "Evaluation of EUV scatterometry for CD characterization of EUV masks using rigorous FEM-Simulation," *Proc. SPIE* **6921**, 69213R (2008).

Ronald Dixson is a staff scientist in the Physical Measurement Laboratory of the National Institute of Standards and Technology (NIST) where he has worked for the past 16 years. His research is primarily on atomic force microscope (AFM) dimensional metrology and standards development at NIST, including the NIST calibrated atomic force microscope (C-AFM) project. Beginning in late 2001, he spent three years as the first NIST guest scientist at SEMATECH where he developed a CD-AFM based reference measurement system (RMS) and utilized this system for the 2004 release of single crystal critical dimension reference materials (SCCDRM) to SEMATECH member companies. His current research interests are calibration methods, traceability, and uncertainty analysis in AFM dimensional metrology. He holds a PhD in physics from Yale University.

Don Chernoff is president and founder of Advanced Surface Microscopy, an independent analytical research and testing laboratory, and a leading commercial supplier of traceable calibration standards for scanned probe microscopes (SPM). His process to accurately measure the size, shape, and position of features in AFM and SEM images helped make DVD possible and supports more than half the world's production of DVD and Blu-Ray disks. He discovered that phase imaging in atomic force microscopy provides important and useful contrast between material domains on surfaces, another technique used worldwide. Earlier, he worked in laser spectroscopy, chemical physics, and electron microscopy. Chernoff was educated at the University of Chicago (BS in chemistry, PhD in physical chemistry).

Shihua Wang works as a senior metrologist in the Optical Metrology Department of the National Metrology Centre (NMC) of Agency for Science, Technology and Research (A*STAR). He is currently involved in the length and dimensional calibration and measurement in both micro- and nano-scale, particularly in carrying out nano-scale measurements using a large range metrological atomic force microscope (LRM-AFM). He received his BEng, MEng, and PhD degrees in 1987, 1990, and 1996, respectively, from the Sichuan University, China. Prior to joining NMC in 2005, he worked as a research fellow in the Department of Mechanical and Production Engineering, National University of Singapore and a lecturer and associate professor in Sichuan University, China. His main research and development interests are in laser interferometric surface profiler, length and dimensional measurements, light scattering surface roughness measurement, and micro(opto)electromechanical systems [ME(O)MS] testing and optics-mechanical design. He has published over 60 journal and conference papers.

Theodore Vorburger was the head of the Surface and Microform Metrology Group in the Precision Engineering Division at the National Institute of Standards and Technology prior to his retirement in 2009. He has since continued as a guest researcher in the group. His areas of scientific interest are traceable surface roughness and step height calibrations, which underpin the national measurement system for surface finish. He led the development of a calibrated atomic force microscope for nano-scale length calibrations and the development of a light scattering system for measuring surface roughness and has collaborated in the development of the world's first sinusoidal-roughness standard reference materials. His current research primarily involves the surface metrology and related physical standards for ballistics materials. He is a member and former chair of the American Society of Mechanical Engineers Standards Committee B46 on the classification and designation of surface qualities. Vorburger has been working in surface metrology since 1976 and is the author or coauthor of approximately 200 publications. He has also served as the chief editor of the Journal of Research of NIST. He holds a PhD in physics from Yale University.

Downloaded from SPIE Digital Library on 14 Mar 2011 to 98.226.79.148. Terms of Use: http://spiedl.org/terms

Siew-Leng Tan is the Head of the Optical Metrology Department of the National Metrology Centre of A*STAR (Agency for Science, Technology, and Research). Her main responsibility is to oversee the metrology areas in length and dimensional, photometry and radiometry, and time and frequency. Siew Leng Tan holds an honors in physics and a master's in the management of technology, both from the National University of Singapore. She has over 20 years of expertise in the length and dimensional metrology. She represents Singapore in the International Committee for Weights and Measures (CIPM) Consultative Committee for Length and its working groups. She is the chair of the Asia Pacific Metrology Programme (APMP) Technical Committee for Length (TCL). Apart from being a technical assessor for the Singapore Laboratory Accreditation Scheme, she is also involved in many calibration and measurement capability (CMC) intra/inter-regional metrology organization (RMO) reviews and peer assessments for other national metrology institutes.

Ndubuisi G. Orji is a mechanical engineer in the Physical Measurement Laboratory of the National Institute of Standards and Technology (NIST). From 2005 to 2008, he was the second NIST guest scientist at SEMATECH where he worked on applications of scanning probe microscopy techniques in semiconductor manufacturing. His research interests are in atomic force microscopy, surface metrology, nano-scale dimensional metrology, and optical metrology. He holds a PhD in mechanical engineering from the University of North Carolina at Charlotte. Orji is a member of SPIE and the American Society for Precision Engineering.

Joseph Fu is a materials engineer in the Physical Measurement Laboratory at the National Institute of Standards and Technology (NIST). His interests are in UHV scanned probe microscopy, scanning electron microscopy, and AFM. Prior to its decommissioning, he was responsible for the NIST metrology electron microscope (MEM), the first SEM to incorporate displacement interferometry. Using this instrument, he oversaw six releases of SRM484, the first traceable SEM magnification standard. He holds a MS in Materials Engineering from the University of Pennsylvania. Fu is an active member of the American Vacuum Society.

Downloaded from SPIE Digital Library on 14 Mar 2011 to 98.226.79.148. Terms of Use: http://spiedl.org/terms